January 2014

Altered ceramide acyl chain length and ceramide synthase gene expression in Parkinson's disease

Sarah Abbott
University of Wollongong, sarahmac@uow.edu.au

Hongyun Li
University of Wollongong, hongyun@uow.edu.au

Sonia Sanz Munoz
University of Wollongong, soniasm@hotmail.com

Bianca Knoch
University of Wollongong, bs567@uowmail.edu.au

Marijka Batterham
University of Wollongong, marijka@uow.edu.au

See next page for additional authors

Altered ceramide acyl chain length and ceramide synthase gene expression in Parkinson's disease

Abstract

Genetic studies have provided increasing evidence that ceramide homeostasis plays a role in neurodegenerative diseases including Parkinson's disease (PD). It is known that the relative amounts of different ceramide molecular species, as defined by their fatty acyl chain length, regulate ceramide function in lipid membranes and in signaling pathways. In the present study we used a comprehensive sphingolipidomic case-control approach to determine the effects of PD on ceramide composition in postmortem brain tissue from the anterior cingulate cortex (a region with significant PD pathology) and the occipital cortex (spared in PD), also assessing mRNA expression of the major ceramide synthase genes that regulate ceramide acyl chain composition in the same tissue using quantitative PCR. In PD anterior cingulate cortex but not occipital cortex, total ceramide and sphingomyelin levels were reduced from control levels by 53% ($P < 0.001$) and 42% ($P < 0.001$), respectively. Of the 13 ceramide and 15 sphingomyelin molecular lipid species identified and quantified, there was a significant shift in the ceramide acyl chain composition toward shorter acyl chain length in the PD anterior cingulate cortex. This PD-associated change in ceramide acyl chain composition was accompanied by an upregulation of ceramide synthase-1 gene expression, which we consider may represent a response to reduced ceramide levels. These data suggest a significant shift in ceramide function in lipid membranes and signaling pathways occurs in regions with PD pathology. Identifying the regulatory mechanisms precipitating this change may provide novel targets for future therapeutics.

Keywords

Parkinson's disease, ceramide, sphingomyelin, ceramide synthase genes, sphingolipidomics, postmortem tissue analysis

Disciplines

Medicine and Health Sciences

Publication Details

Abbott, S. K., Li, H., Sanz Munoz, S., Knock, B., Batterham, M., Murphy, K. E., Halliday, G. M. & Garner, B. (2014). Altered ceramide acyl chain length and ceramide synthase gene expression in Parkinson's disease. Movement Disorders, 29 (4), 518-526.

Authors

Sarah Abbott, Hongyun Li, Sonia Sanz Munoz, Bianca Knoch, Marijka Batterham, Karen E. Murphy, Glenda M. Halliday, and Brett Garner

Final draft version 3 July 2013

Altered ceramide acyl chain length and ceramide synthase gene expression in Parkinson's disease

Sarah K. Abbott [1,2]*, Hongyun Li [1,2], Marijka Batterham [3], Glenda M. Halliday [4,5], Brett Garner [1,2]*

[1]Illawarra Health and Medical Research Institute, University of Wollongong, Wollongong NSW 2522, Australia; [2]School of Biological Sciences, University of Wollongong, Wollongong NSW 2522, Australia; [3]National Institute of Applied Statistics Research Australia, University of Wollongong, Wollongong NSW 2522, Australia; [4] Neuroscience Research Australia; Sydney, NSW 2031, Australia; [5] School of Medical Sciences, University of New South Wales, Sydney, NSW 2031, Australia.

Running title: Altered ceramide in Parkinson's disease

Key words: Parkinson's disease, ceramide, sphingomyelin, ceramide-synthase, sphingolipidomics, postmortem-tissue-analysis

* Correspondence to: Dr Sarah Abbott, Illawarra Health and Medical Research Institute, University of Wollongong, NSW 2522, Australia, Email: sarahmac@uow.edu.au; Tel: +61 2 4298 1997; Fax: +61 2 4221 8130, or Prof Brett Garner, Illawarra Health and Medical Research Institute, University of Wollongong, NSW 2522, Australia; Email: brettg@uow.edu.au; Tel: +61 2 4298 1576; Fax: +61 2 4221 8130

ABSTRACT **(237/250 words)**

Genetic studies have provided increasing evidence that ceramide homeostasis plays a role in neurodegenerative diseases including Parkinson's disease (PD). It is known that the relative amounts of different ceramide molecular species, as defined by their fatty acyl chain length, regulate ceramide function in lipid membranes and in signaling pathways. For this reason we used a comprehensive sphingolipidomic case-control approach to determine the effects of PD on ceramide composition in postmortem brain tissue from the anterior cingulate cortex (ACC, a region with significant PD pathology) and the occipital cortex (OCC, spared in PD), also assessing mRNA expression of the major CerS genes that regulate ceramide acyl chain composition in the same tissue using quantitative PCR. In PD ACC but not OCC, total ceramide and sphingomyelin levels were reduced from control levels by 53% ($p < 0.001$) and 42% ($p < 0.001$) respectively. Of the 13 ceramide (d18:1) and 15 sphingomyelin (d18:1) molecular lipid species identified and quantified, there was a significant shift in the ceramide acyl chain composition towards shorter acyl chain length in the PD ACC. This PD-associated change in ceramide acyl chain composition was accompanied by an upregulation of CerS1 gene expression, which we consider may represent a response to reduced ceramide levels. These data suggest a significant shift in ceramide function in lipid membranes and signalling pathways occurs in regions with PD pathology. Identifying the regulatory mechanisms precipitating this change may provide novel targets for future therapeutics.

INTRODUCTION

Parkinson's disease (PD) is a neurodegenerative movement disorder with a prevalence of approximately 1-2% of the population over 65 years increasing to 3-5% in people over 85 years old [1, 2]. The pathological hallmarks of PD include the specific loss of dopaminergic neurons in the substantia nigra pars compacta (SN) and the formation of Lewy bodies and Lewy neurites that are composed of aggregated alpha-synuclein (α-syn) protein and other components including lipids [3-5]. Lewy pathologies occur progressively in a proportion of selective neurons located in the brainstem, temporal mesocortex and neocortex [3, 6-8]. Severe destruction of the SN and involvement of the amygdala and the anterior cingulate cortex (ACC) occur relatively early after the onset of clinical symptoms, whereas the occipital cortex is pathologically spared [3, 6-8].

There has been a recent surge of interest in the role that altered sphingolipid homeostasis may play in neurodegenerative diseases including PD [9-14]. Ceramide is a component of all major sphingolipid species in the brain including sphingomyelins (SMs) and glycosphingolipids (GSLs) and also plays a crucial role in regulating cellular membrane structure, in apoptosis and as a signaling molecule after its phosphorylation by ceramide kinase [15-20]. The ceramide molecule comprises a sphingoid base to which one of several distinct fatty acid species is attached through an *N*-acyl linkage. The *N*-acylation reaction is mediated by a family of ceramide synthase (CerS) enzymes (CerS1-6) that each utilize a different restricted subset of fatty acyl CoA species [20].

Ceramide may be generated through three main pathways (**Fig 1**): (i) *de novo* synthesis beginning with serine and palmitoyl-CoA, (ii) via the breakdown of sphingomyelin by sphingomyelinase, and (iii) by the breakdown of glucosylceramide by glucosylceramidase

(GCase) [21]. The latter route for ceramide production, also known as the salvage pathway, is the most energy efficient mechanism for ceramide generation in post-mitotic cells and is thought to account for 50% to 90% of sphingolipid production depending on the lipid molecular species and the cell type [22, 23]. Any pathological changes that impair the salvage pathway could therefore eventually have an impact on cellular membrane structure and signalling pathways [22-24]. It is highly relevant that mutations in the *GBA* gene (that encodes GCase) confer increased risk for PD [25-27]. Intriguingly, GCase levels and activity are reduced in several brain regions in both sporadic PD and PD cases carrying *GBA* mutations as compared to healthy controls [28]. *In vitro* studies suggest that increased α-syn levels may impair GCase trafficking and also decrease its enzyme activity [28, 29]. Overall, the prediction would be that these changes in GCase levels and/or activity would reduce cerebral ceramide levels in PD.

In the context of the function of ceramide in the brain and in neurodegenerative diseases, it is clear that it is not only the overall amount of ceramide that is important, but the relative amounts of the different ceramide molecular species as defined by their fatty acyl chain length. For example, changes in ceramide fatty acyl chain length can affect membrane order, membrane lipid peroxidation, mitochondrial function and apoptotic pathways in a distinct manner [14, 30-33]. There are currently only limited data available regarding how cerebral ceramide acyl chain composition may change in PD and no data on how this may correlate with the expression of the CerS genes that control this diversity of ceramide molecular species.

In the current study we have used a sphingolipidomics case-control approach to determine the effects of PD on ceramide composition in postmortem brain tissue from the anterior cingulate

cortex (ACC) and the occipital cortex (OCC). None of the cases or controls analysed in this study had known *GBA* mutations. The expression of the major CerS genes in the brain was also assessed at the mRNA level using quantitative PCR (qPCR).

MATERIALS AND METHODS

Materials

Methyl-*tert*-butyl ether (MTBE), chloroform and methanol were HPLC grade and purchased from Thermo Scientific, Scoresby, VIC, Australia. Analytical grade butylated hydroxytoluene (BHT) and sodium hydroxide (98% minimum) were from Sigma Aldrich, Sydney, NSW, Australia and analytical grade ammonium acetate was from Crown Scientific, Moorebank, NSW, Australia. Screw thread vials (4 mL) and wide mouth vials (1.8 mL) with PTFE/silicone septa caps were from Grace Davison, Rowville, VIC, Australia. The internal standard mixture contained 75 μM CerPCho(d18:0/12:0) and 75 μM Cer(d18:1/10:0) in chloroform/methanol (2:1, vol:vol); Avanti Polar Lipids purchased from Auspep, Tullamarine, VIC, Australia.

Human Brain Tissue

Frozen brain grey matter and white matter samples from 10 control cases and 9 sporadic PD cases were received from the Sydney Brain Bank and the NSW Tissue Resource Centre. Standardized clinicopathological criteria were used for diagnosis with no case or control having any evidence of significant neuropathology other than PD [34]. The cohorts were matched for both age (PD 77.8 $\pm$ 1.9 y, controls 74.7 $\pm$ 2.9 y, mean $\pm$ SE) and postmortem interval (Con 22.0 $\pm$ 4.8 h, PD 18.4 $\pm$ 2.9 h, mean $\pm$ SE) and an absence of common *GBA* mutations that account for 70% of causative GD alleles in non-Jewish populations (GM Halliday and E Sidransky, unpublished data). These variables will not be evaluated further.

Full demographic details are provided in **Table 1**. Ethics approval was from the University of New South Wales Human Research Ethics Committee and the University of Wollongong Human Research Ethics Committee. Approximately 100 mg of frozen brain tissue from the ACC and OCC was pulverized over dry ice and two aliquots of approximately 50 mg were accurately weighed stored at -80°C until required for lipid or qPCR analysis.

Sphingolipid extraction and analysis by mass spectrometry

The lipid extraction and mass spectrometry analysis was performed as previously described in detail [35]. In brief, approximately 15 mg of pulverised human brain tissue was accurately weighed directly into each 0.5 mL Precellys® tube (Sapphire Bioscience, Waterloo, NSW, Australia) and homogenised in 300 µL ice-cold methanol containing internal standards (4 µL /mg tissue) and BHT (0.01% w/v), using a Precellys®24 bead homogeniser (Bertin Technologies; 2 x 30 sec at 6000 rpm). After transferring the homogenate to a 4 mL glass vial, the Precellys tube was rinsed with 162 µL methanol and 1540 µL MTBE was added to the glass vial (final MTBE/methanol ratio 10:3, vol:vol). Following overnight extraction/hydrolysis (with 0.7M sodium hydroxide), 253 µL of 0.15M ammonium acetate was added and the organic (upper) phase was collected in a 4 mL vial. The original homogenate was re-extracted by addition of 205 µL of the upper phase MTBE/methanol/0.15M ammonium acetate and combining the upper phase with the first extract. This lipid extract was then dried under nitrogen at 37°C and resuspended in chloroform/methanol (1:2, vol:vol).

The lipid extracts were analysed via ESI-MS using a hybrid triple quadrupole ion trap mass spectrometer (QTRAP® 5500, AB SCIEX, Framingham, Massachusetts, USA) and an attached chip-based, automated nanospray source (Triversa Nanomate®, Advion, Ithaca, NY,

USA). Sphingolipid species were quantified using AB SCIEX Lipidview™ Software (Framingham, Massachusetts, USA; see [36]) as described previously [35]. The processing settings for Lipidview™ were: mass tolerance 0.5, minimum % intensity 0 and minimum S/N 50.

RNA extraction and ceramide synthase analysis by qPCR

The qPCR analysis of human brain samples was performed as described previously [37] with minor modifications. In brief, approximately 30 mg of pulverised human brain tissue was accurately weighed directly into each 0.5 mL Precellys® tube (Sapphire Bioscience, Waterloo, NSW, Australia) and homogenised in 300 μL TRI reagent using a Precellys®24 bead homogeniser (Bertin Technologies) with the following settings: 2 x 10 sec at 5500 rpm with 10 sec break (based on recommendations from Bertin Technologies). The RNA concentration was determined spectrophometrically with a Nanodrop 1000 (Thermo scientific, Wilmington, DE). Two μg of total RNA was used for reverse transcription with oligo dT(18) primer according to the instructions provided with the Tetro cDNA Synthesis kit (Bioline, Sydney, Australia). Quantitative real-time PCR was carried out in a Roche Lightcycler® 480 real-time PCR system using SensiFAST SYBR No-ROX kit (Bioline, Sydney, Australia), following the manufacturer's protocol. Analyses were performed in duplicate, and CerS gene expression was normalised to cyclophilin A mRNA levels. The level of expression for each gene was calculated using the comparative threshold cycle (Ct) value method using the formula $2^{-\Delta\Delta Ct}$ (where $\Delta\Delta Ct = \Delta Ct$ sample $- \Delta Ct$ reference) as described previously [38].

All primers were purchased from Sigma (Castle Hill, Australia) and details of the sequences are as follows: Cyclophilin A (F: AGGGTTCCTGCTTTCACAGA and R:

GTCTTGGCAGTGCAGATGAA), CerS1 (F: ACGCTACGCTATACATGGACAC and R: AGGAGGAGACGATGAGGATGAG), CerS2 (F: CCGATTACCTGCTGGAGTCAG and R: GGCGAAGACGATGAAGATGTTG), CerS4 (F: CTTCGTGGCGGTCATCCTG and R: TGTAACAGCAGCACCAGAGAG), CerS5 (F: GCCATCGGAGGAATCAGGAC and R: GCCAGCACTGTCGGATGTC) and CerS6 (F: GGGATCTTAGCCTGGTTCTGG and R: GCCTCCTCCGTGTTCTTCAG).

Statistical analyses

Statistical analyses were performed using SPSS Statistics v19.0.0 (IBM, NY, USA). All results are expressed as mean ± standard error with $p < 0.05$ set as the level of significance. Group data were tested for normality using Shapiro-Wilk W test and homogeneity of variance using a 2-sided F Test. Multivariate analysis of covariance was used to assess the significance of the difference between PD and control with acyl chain structure by region as the dependent variable, case as the group variable and age and post mortem interval as covariates. The analysis of the mRNA data was conducted using a linear mixed model. To control for multiple comparisons additional post hoc comparisons were conducted using the method of Benjamini and Hochberg [39], these analyses were conducted using the p.adjust command in the package "stats" in R version 2.15.2 (R Core Development Team)[40].

RESULTS

Ceramide analysis

As ceramide concentration and acyl chain composition are postulated to be important in neurodegenerative diseases [9, 30], we conducted a detailed analysis of the major ceramide molecular species in human control and PD brain samples. A quantitative (nmol/g tissue wet

weight) comparison between control and PD ceramide species for grey matter samples obtained from the ACC and OCC is shown in **Table 2**. A total of 13 ceramide species were detected in both regions, with fatty acyl chain lengths ranging from C16 – C26. The total ceramide concentration in the PD ACC was significantly lower (53%) than in the control ACC. Significant reductions in most individual ceramide species were observed in the PD ACC samples. The greatest reductions were detected in Cer(d18:1/22:0), Cer(d18:1/23:0) and Cer(d18:1/24:1) with approximately 60% lower levels in PD relative to control. In contrast, no significant changes in the concentration of any ceramide species were detected when the OCC samples were compared. While there were more males in the PD cohort (n = 7) compared to the control cohort (n = 5), analysis of the sphingolipidomic mass spectrometry data for an influence of gender revealed there were no significant differences (SK Abbott and B Garner, unpublished data). The gender of the cohorts is therefore unlikely to confound the disease-status comparisons.

In order to directly compare the distribution of ceramide fatty acyl chains in the control and PD samples, the data were also expressed in units of mol % (**Fig 2**). As expected [41], by far the two most abundant ceramide species detected in both the ACC and OCC were Cer(d18:1/18:0) and Cer(d18:1/24:1). Importantly, this analysis revealed a significant increase in C18:0 acyl chain content accompanied by a significant decrease in C24:1 acyl chain content in the PD ACC compared to control ACC (**Fig 2**). These changes remained significant when adjustment was made for multiple comparisons (P = 0.026 for both comparisons). This change in ceramide acyl composition was not present in the OCC sample comparison. There were additional quantitatively minor changes in acyl chain composition in the PD ACC compared to control ACC, overall indicating a shift from longer to shorter ceramide acyl chain composition in the PD cohort (**Fig 2**).

Sphingomyelin analysis

We also analysed SM concentration and acyl chain composition in the same grey matter samples used for the ceramide analysis described above. Similar to the ceramide results, total SM levels were significantly decreased (42%) in the PD ACC compared to the control ACC, whereas there were no significant differences observed when the SM content of the control OCC and PD OCC were compared (**Supplementary Table 1**). When assessing SM acyl chain composition using a mol % analysis, several significant differences were revealed. Notably, in the PD ACC significant decreases in C23:0, C24:1 and C26:1 were observed and these were accompanied by significantly increased C18:1 and C20:0 levels (and a non-significant trend for a 15% increase in C18:0) as compared to the control ACC. Similar to the changes in ceramide acyl chain composition, the SM data in general also suggest a shift from longer to shorter acyl chain composition in the PD cohort.

SM is present in the cellular membranes of all brain cell types, however, the vast majority of SM in the brain is within myelin. Since white matter is highly enriched in myelin, and thus myelin lipids, we conducted an additional assessment of white matter samples derived from both the ACC and OCC of control samples and PD cases. The PD-associated changes in ceramide and SM absolute amounts and acyl chain length we detected in the grey matter ACC samples were not replicated in the white matter ACC (**Supplementary Table 2 and 3**). This suggests that the grey matter ACC changes are unlikely to be due to myelin lipid changes. Interestingly, we detected a significant decrease in several white matter ceramide and SM species in the PD OCC compared to the control OCC (**Supplementary Table 2 and 3**).

Ceramide synthase gene expression

In order to examine a possible underlying cause of the shift from longer to shorter ceramide acyl chain composition in grey matter samples from the PD ACC cohort, we next examined grey matter samples for the expression of the 5 CerS (*LASS*) genes that are expressed in the human brain (CerS1, CerS2, CerS4, CerS5 and CerS6). CerS1 and CerS4 preferentially attach C18 and C20 fatty acyl chains to dihydrosphinganine to form C18 and C20 dihydroceramides. These dihydroceramides are then converted to C18 and C20 ceramides via dihydroceramide desaturase [14]. The expression of CerS1 and CerS4 mRNA was significantly increased by approximately 2-fold and 3-fold, respectively, in the PD ACC compared to the control ACC (**Fig 3**). After correction for multiple comparisons the differences in CerS1 remained significant whereas the differences in CerS4 were no longer signficiant (**Fig 3**). The change in ACC CerS gene expression is consistent with the PD-associated increases in C18, C20 and C16 ceramide species we detected using the sphingolipidomics analysis described above. There was no significant change in CerS2 mRNA levels in the PD ACC compared to the control ACC (**Fig 3**). CerS2 is predicted to control the synthesis of C24 ceramides in the brain. It is therefore plausible that the lack of change in CerS2 accompanied by increases in CerS1 contributes to the changes in ceramide (and SM) acyl chain composition we detected in the PD ACC (**Fig 2**).

In contrast to the PD-associated changes in CerS gene expression in the ACC, we did not detect an increase in CerS mRNA in the PD OCC (**Fig 3**). This is again consistent with the lack of significant changes in ceramide acyl chain length in the PD OCC compared to the control OCC (**Fig 2**). For reasons that remain unclear, in the PD OCC CerS5 expression was reduced. A non-significant trend for increased Cer6 expression might be predicted to result in

no net change in ceramide acyl chain composition as CerS5 and CerS6 have overlapping substrate specificity (e.g. for C16 fatty acyl CoA).

Discussion

Although a strong rationale has been provided suggesting that altered ceramide metabolism may contribute to PD [9-14], there is very little data available regarding the molecular structure and levels of post-mortem brain ceramides in PD patients. In the present study we show that overall grey matter ceramide and SM levels are reduced in PD ACC, a brain region that contains Lewy body pathology from around Braak Stage IV onwards [3, 6-8]. In contrast, such reductions in ceramide and SM were not observed in the PD OCC, a brain region that is spared PD pathology; although in the latter case, changes in white matter sphingolipids were observed. As ceramide acyl chain structure has a major influence on the biological function of this class of lipids [14, 30-33], it is also highly significant that our data revealed for the first time a shift in ceramide acyl chain composition, with PD ACC ceramide species containing more short chain ceramides (e.g. C16:0, C18:0 and C18:1) at the expense of long chain ceramides (e.g. C23:0 and C24:1). What drives these changes cannot be determined from this (or any) post-mortem study; however, based on previous work and our current analysis of CerS mRNA expression, we provide one plausible mechanistic explanation.

As noted above, a major source of ceramide generation in the brain is thought to be via the salvage pathway. There is strong evidence that reduced GCase levels and activity are associated with PD [25-29] and, consistent with the data presented herein, this would be predicted to lead to a reduction in total ceramide levels in affected PD brain tissue. This loss

of GCase activity may indeed underlie the association of *GBA* mutations with increased PD risk. Interactions between GCase activity, α-synuclein and PINK1 have also been proposed to modulate ceramide metabolism in PD [29, 42]. Intriguingly, recent data suggests that a number of additional genes associated with Lewy body pathology may also play a role in ceramide metabolism [9]. For example, *PANK2* and *PLA2G6*, which encode pantothenate kinase and phospholipase A_2, respectively, are associated with two neurodegenerative disorders (Neurodegeneration with brain iron accumulation 1 and 2) that have Lewy body inclusions [9]. Pantothenate kinase regulates CoA biosynthesis and phospholipase A_2 activation promotes SMase-mediated generation of ceramide from SM [43]. It is also possible to link *LRRK2* mutations with ceramide metabolism in PD as mutant LRRK2 interaction with parkin induces neuron death [44], most likely by inhibiting the normal function of parkin in preventing ceramide-induced cell death [45]. Overall, these studies highlight that there are a number of pathways associated with PD that are predicted to result in altered ceramide metabolism and potentially reduced ceramide levels in affected PD brain tissue.

The abovementioned examples do not, however, provide a mechanistic explanation for the alterations in ceramide acyl chain composition that we have detected. The simplest explanation for the shift in ceramide acyl chain composition, with increased short-chain ceramides and decreased long-chain ceramides in PD, is that a homeostatic response to reductions in ceramide generated through the salvage pathway is evoked in PD. This postulated activation of *de novo* synthesis is supported by the selective increases in specific CerS genes in the PD tissues that match the observed changes in ceramide acyl chain compositions. For reasons that remain to be defined, the induction of CerS gene expression in the PD ACC did not match the expression of these genes in the control brain tissues (e.g. in the PD ACC we observed a 2-fold upregulation CerS1 with no significant change in CerS2).

Regardless of the reason for the preferential induction of specific CerS genes in the PD brain, the consequent shift in ceramide acyl chain content may have physiological consequences. Although it is tempting to speculate that the PD-associated increase in short acyl chain ceramides may promote cellular apoptosis [32], the fact that the overall ceramide concentrations are reduced may to a degree circumvent this. A decrease in ceramide acyl chain length could also have an impact on membrane lipid order, lipid-lipid and lipid-protein interactions, signalling pathways and potentially on membrane lipid peroxidation reactions [12, 24, 46-48]. In a previous study using an independent cohort of control and PD samples we conducted a broad liquid chromatography – mass spectrometry (LC-MS) lipidomics analysis of late stage (7/10 PD cases were Braak stage V) PD ACC samples [37]. In this earlier analysis we were able to accurately quantify 6 Cer(d18:1) molecular species. Interestingly, this earlier study also indicted an increase in the relative distribution of Cer(d18:1/18:0) and Cer(d18:1/20:0) in the ACC but not in OCC [37]. The functional implications that altered ceramide acyl chain composition may have in PD neurodegeneration therefore appear to be worth exploring in future studies.

In summary, we have shown that decreased levels of ceramide occur selectively in a brain region with PD pathology. This may be due to an impairment of the salvage pathway for ceramide generation that is not adequately compensated for by upregulated *de novo* synthesis. Induction of CerS1 gene expression in the same affected region with PD may represent a response to the reduced ceramide levels. The specific pattern of CerS gene induction detected matches the alterations in ceramide acyl chain structures we detected in the PD tissues. Altered ceramide metabolism occurs in PD and may play an important but as yet undefined functional role in the ongoing neurodegeneration observed.

Acknowledgments

Tissues were received from the Sydney Brain Bank at Neuroscience Research Australia and the New South Wales Tissue Resource Centre at the University of Sydney which are supported by the National Health and Medical Research Council of Australia (NHMRC), University of New South Wales, Neuroscience Research Australia, Schizophrenia Research Institute and National Institute of Alcohol Abuse and Alcoholism (NIH (NIAAA) R24AA012725). The work was supported by NHMRC project grant (#1008307). BG is an ARC Future Fellow (#FT0991986) and NHMRC Senior Research Fellow (Hon, #630445). GMH is an NHMRC Senior Principal Research Fellow (#630434).

Funding agencies

This research was supported by the National Health & Medical Research Council of Australia (#1008307 to Glenda M. Halliday and Brett Garner, #630434 to Glenda M. Halliday, and #630445 to Brett Garner); and the Australian Research Council (FT0991986 to Brett Garner).

Relevant conflicts of interest/financial disclosures

Nothing to report.

Author Roles

Dr Abbott: Research project organization and execution. Statistical analysis review and critique. Manuscript preparation writing of the first draft, review and critique. Dr Li: Research project organization and execution. Manuscript preparation review and critique. Dr Batterham: Statistical analysis: design, execution, review and critique. Manuscript preparation review and critique. Dr Halliday: Research project: conception and organization. Statistical analysis: design, review and critique. Manuscript preparation: review and critique. Dr Garner: Research project: conception and organization. Statistical analysis: review and critique. Manuscript preparation: writing of the first draft, review and critique.

REFERENCES

1. Fahn S. Description of Parkinson's disease as a clinical syndrome. Ann N Y Acad Sci 2003;991:1-14.
2. Obeso JA, Rodriguez-Oroz MC, Goetz CG, et al. Missing pieces in the Parkinson's disease puzzle. Nat Med 2010;16(6):653-661.
3. Dickson DW, Braak H, Duda JE, et al. Neuropathological assessment of Parkinson's disease: refining the diagnostic criteria. Lancet Neurol 2009;8(12):1150-1157.
4. Gai WP, Yuan HX, Li XQ, Power JT, Blumbergs PC, Jensen PH. In situ and in vitro study of colocalization and segregation of alpha-synuclein, ubiquitin, and lipids in Lewy bodies. Exp Neurol 2000;166(2):324-333.
5. Halliday GM, Ophof A, Broe M, et al. Alpha-synuclein redistributes to neuromelanin lipid in the substantia nigra early in Parkinson's disease. Brain 2005;128(Pt 11):2654-2664.
6. Braak H, Del Tredici K, Rub U, de Vos RA, Jansen Steur EN, Braak E. Staging of brain pathology related to sporadic Parkinson's disease. Neurobiol Aging 2003;24(2):197-211.
7. Dickson DW, Fujishiro H, Orr C, et al. Neuropathology of non-motor features of Parkinson disease. Parkinsonism Relat Disord 2009;15 Suppl 3:S1-5.
8. Halliday GM, McCann H. The progression of pathology in Parkinson's disease. Ann N Y Acad Sci 2010;1184:188-195.
9. Bras J, Singleton A, Cookson MR, Hardy J. Emerging pathways in genetic Parkinson's disease: Potential role of ceramide metabolism in Lewy body disease. FEBS J 2008;275(23):5767-5773.

10. Haughey NJ. Sphingolipids in neurodegeneration. Neuromolecular Med 2010;12(4):301-305.

11. Haughey NJ, Bandaru VV, Bae M, Mattson MP. Roles for dysfunctional sphingolipid metabolism in Alzheimer's disease neuropathogenesis. Biochim Biophys Acta 2010;1801(8):878-886.

12. Fabelo N, Martin V, Santpere G, et al. Severe alterations in lipid composition of frontal cortex lipid rafts from Parkinson's disease and incidental Parkinson's disease. Mol Med 2011;17(9-10):1107-1118.

13. Zhao L, Spassieva SD, Jucius TJ, et al. A Deficiency of Ceramide Biosynthesis Causes Cerebellar Purkinje Cell Neurodegeneration and Lipofuscin Accumulation. PLoS Genet 2011;7(5):e1002063.

14. Grösch S, Schiffmann S, Geisslinger G. Chain length-specific properties of ceramides. Progress in Lipid Research 2012;51(1):50-62.

15. Kolesnick RN, Kronke M. Regulation of ceramide production and apoptosis. Annu Rev Physiol 1998;60:643-665.

16. Silva LC, Ben David O, Pewzner-Jung Y, et al. Ablation of ceramide synthase 2 strongly affects biophysical properties of membranes. J Lipid Res 2012;53(3):430-436.

17. Morales A, Lee H, Goñi F, Kolesnick R, Fernandez-Checa J. Sphingolipids and cell death. Apoptosis 2007;12(5):923-939.

18. Movsesyan VA, Yakovlev AG, Dabaghyan EA, Stoica BA, Faden AI. Ceramide induces neuronal apoptosis through the caspase-9/caspase-3 pathway. Biochemical and Biophysical Research Communications 2002;299(2):201-207.

19. Chalfant CE, Spiegel S. Sphingosine 1-phosphate and ceramide 1-phosphate: expanding roles in cell signaling. J Cell Sci 2005;118(Pt 20):4605-4612.

20. Mencarelli C, Martinez–Martinez P. Ceramide function in the brain: when a slight tilt is enough. Cellular and Molecular Life Sciences 2013;70(2):181-203.

21. Kitatani K, Idkowiak-Baldys J, Hannun YA. The sphingolipid salvage pathway in ceramide metabolism and signaling. Cellular Signalling 2008;20(6):1010-1018.

22. Gillard BK, Clement RG, Marcus DM. Variations among cell lines in the synthesis of sphingolipids in de novo and recycling pathways. Glycobiology 1998;8(9):885-890.

23. Tettamanti G, Bassi R, Viani P, Riboni L. Salvage pathways in glycosphingolipid metabolism. Biochimie 2003;85(3–4):423-437.

24. Soreghan B, Thomas SN, Yang AJ. Aberrant sphingomyelin/ceramide metabolic-induced neuronal endosomal/lysosomal dysfunction: potential pathological consequences in age-related neurodegeneration. Adv Drug Deliv Rev 2003;55(11):1515-1524.

25. DePaolo J, Goker-Alpan O, Samaddar T, Lopez G, Sidransky E. The association between mutations in the lysosomal protein glucocerebrosidase and parkinsonism. Mov Disord 2009;24(11):1571-1578.

26. Mitsui J, Mizuta I, Toyoda A, et al. Mutations for Gaucher disease confer high susceptibility to Parkinson disease. Arch Neurol 2009;66(5):571-576.

27. Sidransky E, Nalls MA, Aasly JO, et al. Multicenter analysis of glucocerebrosidase mutations in Parkinson's disease. N Engl J Med 2009;361(17):1651-1661.

28. Gegg ME, Burke D, Heales SJ, et al. Glucocerebrosidase deficiency in substantia nigra of parkinson disease brains. Ann Neurol 2012;72(3):455-463.

29. Mazzulli JR, Xu YH, Sun Y, et al. Gaucher disease glucocerebrosidase and alpha-synuclein form a bidirectional pathogenic loop in synucleinopathies. Cell 2011;146(1):37-52.

30. Ben-David O, Futerman AH. The Role of the Ceramide Acyl Chain Length in Neurodegeneration: Involvement of Ceramide Synthases. NeuroMolecular Medicine 2010;12(4):341-350.

31. Levy M, Futerman AH. Mammalian ceramide synthases. IUBMB Life 2010;62(5):347-356.

32. Sassa T, Suto S, Okayasu Y, Kihara A. A shift in sphingolipid composition from C24 to C16 increases susceptibility to apoptosis in HeLa cells. Biochim Biophys Acta 2012;1821(7):1031-1037.

33. Mullen TD, Hannun YA, Obeid LM. Ceramide synthases at the centre of sphingolipid metabolism and biology. Biochemical Journal 2012;441(3):789-802.

34. Halliday G, Ng T, Rodriguez M, et al. Consensus neuropathological diagnosis of common dementia syndromes: testing and standardising the use of multiple diagnostic criteria. Acta Neuropathol 2002;104(1):72-78.

35. Abbott SK, Jenner AM, Mitchell TW, Brown SH, Halliday GM, Garner B. An improved high-throughput lipid extraction method for the analysis of human brain lipids. Lipids 2013;48(3):307-318.

36. Ejsing CS, Duchoslav E, Sampaio J, et al. Automated Identification and Quantification of Glycerophospholipid Molecular Species by Multiple Precursor Ion Scanning. Anal Chem 2006;78(17):6202-6214.

37. Cheng D, Jenner AM, Shui G, et al. Lipid pathway alterations in Parkinson's disease primary visual cortex. PLoS One 2011;6(2):e17299.

38. Li H, Evin G, Hill AF, Hung YH, Bush AI, Garner B. Dissociation of ERK signalling inhibition from the anti-amyloidogenic action of synthetic ceramide analogues. Clin Sci (Lond) 2012;122(9):409-419.

39. Benjamini Y, Hochberg Y. Controlling the false discovery rate: a practical and powerful approach to multiple testing. Journal of the Royal Statistical Society Series B 1995;57:289–300.

40. R Development Core Team. R: A language and environment for statistical computing. R Foundation for Statistical Computing, Vienna, Austria 2008:ISBN 3-900051-900007-900050, URL http://www.R-project.org.

41. Laviad EL, Albee L, Pankova-Kholmyansky I, et al. Characterization of ceramide synthase 2: tissue distribution, substrate specificity, and inhibition by sphingosine 1-phosphate. J Biol Chem 2008;283(9):5677-5684.

42. Manning-Bog AB, Schule B, Langston JW. Alpha-synuclein-glucocerebrosidase interactions in pharmacological Gaucher models: a biological link between Gaucher disease and parkinsonism. Neurotoxicology 2009;30(6):1127-1132.

43. Lei X, Zhang S, Bohrer A, Bao S, Song H, Ramanadham S. The group VIA calcium-independent phospholipase A2 participates in ER stress-induced INS-1 insulinoma cell apoptosis by promoting ceramide generation via hydrolysis of sphingomyelins by neutral sphingomyelinase. Biochemistry 2007;46(35):10170-10185.

44. Smith WW, Pei Z, Jiang H, et al. Leucine-rich repeat kinase 2 (LRRK2) interacts with parkin, and mutant LRRK2 induces neuronal degeneration. Proc Natl Acad Sci U S A 2005;102(51):18676-18681.

45. Darios F, Corti O, Lucking CB, et al. Parkin prevents mitochondrial swelling and cytochrome c release in mitochondria-dependent cell death. Hum Mol Genet 2003;12(5):517-526.

46. Fortin DL, Troyer MD, Nakamura K, Kubo S, Anthony MD, Edwards RH. Lipid rafts mediate the synaptic localization of alpha-synuclein. J Neurosci 2004;24(30):6715-6723.

47. Jana A, Hogan EL, Pahan K. Ceramide and neurodegeneration: susceptibility of neurons and oligodendrocytes to cell damage and death. J Neurol Sci 2009;278(1-2):5-15.

48. Zigdon H, Kogot-Levin A, Park JW, et al. Ablation of ceramide synthase 2 causes chronic oxidative stress due to disruption of the mitochondrial respiratory chain. J Biol Chem 2013;288(7):4947-4956.

FIGURE LEGENDS

Figure 1. Ceramide homeostasis overview. Ceramide may be generated through *de novo* synthesis, beginning with serine and palmitoyl-CoA, or via the salvage pathway that involves the breakdown of sphingomyelin by sphingomyelinase, and the breakdown of glucosylceramide and galactosylceramide by specific glycosylceramidases. Ceramide synthases play a major role in the *de novo* synthesis pathway and also are involved in sphingosine recycling. Reactions contributing to the salvage pathway are indicated by the broken arrows. SPT, serine palmitoyl transferase; 3KR, 3-ketosphinganine reductase; CerS1-6, ceramide synthases 1-6; DES, dihydroceramide desaturase; GCS, glucosylceramide synthase; GCase, glucosyl ceramidase; CGT, ceramide glactosyl transferase; GalC, galactosyl ceramidase; SMase, sphingomyelinase; SMS, sphingomyelin synthase; FA-CoA, fatty acyl CoA; GSL, glycosphingolipid; Glc-ceramide, glucosylceramide; Gal-ceramide, galactosylceramide; S1P, sphingosine-1-phosphate.

Figure 2. Comparison of ceramide acyl chain structure in control and PD brain samples. Control (n = 10) and PD (n = 9) tissues were collected from (A) the anterior cingulate cortex ("ACC") and (B) the occipital cortex ("OCC"). Lipids were extracted and analysed using a sphingolipidomics mass spectrometry approach. The data indicates the relative percentage (mol%) composition that each of the indicated fatty acyl chain structures contributes to the ceramide (d18:1) lipid molecular species. Control samples are indicated by the grey bars and PD samples are indicated by the black bars. Values are mean ± SE. * $P < 0.05$ using a multivariate analysis of covariance with ACC and OCC values as the dependent variable,

case as the grouping variable, and age and post-mortem interval as covariate. When adjusting for multiple comparisons using the Benjamini and Hochberg method all results remain significant with the exception of 20:0, 23:1, and 25:0 in the ACC and the 22:1 is no longer significant in the OCC when the analysis is adjusted for multiple comparisons (#).

Figure 3: **Quantitative real-time PCR analysis of** ceramide synthase mRNA expression in control and PD brain samples. Control (n = 10) and PD (n = 9) tissues were collected from (A) the anterior cingulate cortex ("ACC") and (B) the occipital cortex ("OCC") and the levels of CerS gene expression analysed using qPCR. CerS mRNA levels were calculated relative to housekeeper cyclophylin A mRNA levels. Data for the expression each CerS gene in the PD samples is expressed relative to the control values (assigned a value of 1.0). Control samples are indicated by the grey bars and PD samples are indicated by the black bars. Differences between groups PD and Con were analysed using a linear mixed model to control for covariates and further adjustment for multiple comparisons was conducted using the Benjamini and Hochberg method (in this case the CerS4 is no longer significant in the ACC region (P=0.160) when the analysis is adjusted for multiple comparisons (#). Values are mean ± SE. * $P < 0.05$.

Table 1. Demographic details for control (Con) and Parkinson's disease (PD) cohorts.

Case #	Gender (M/F)	Post-mortem interval (h)	Age at death (y)	PD duration (y)	Braak PD stage (0 – VI)
Con 1	F	40.5	78	-	0
Con 2	F	7.5	82	-	0
Con 3	M	6.5	78	-	0
Con 4	M	25	60	-	0
Con 5	M	13.5	69	-	0
Con 6	M	48	73	-	0
Con 7	F	25	72	-	0
Con 8	M	9	88	-	0
Con 9	F	10	85	-	0
Con 10	F	35	62	-	0
PD 1	M	24[#]	75	n.a.	IV
PD 2	M	24[#]	71	n.a.	IV
PD 3	M	23	80	n.a.	IV
PD 4	F	6	75	10	IV
PD 5	M	24[#]	74	n.a.	IV
PD 6	F	14	74	17	VI
PD 7	M	24[#]	78	36	V
PD 8	M	24[#]	85	8	IV
PD 9	M	3	88	20	IV

[#] Estimated PMI based on date of death and date of brain collection.

[n.a.] Data not available.

Table 2. Ceramide concentrations (nmol/g tissue wet weight) in anterior cingulate cortex (ACC) and occipital cortex (OCC) derived from control (n= 10) and Parkinson's disease (PD) cases (n=9).

Cer(d18:1) acyl chain structure	ACC (Grey matter)			OCC (Grey matter)		
	Control	PD	p	Control	PD	p
16:0	12.5 ± 0.9	11.9 ± 1.3	0.833	14.6 ± 1.5	14.0 ± 2.1	0.857
18:0	445.9 ± 29.5	271.2 ± 43.3	0.018	387.0 ± 40.9	326.2 ± 48.0	0.747
18:1	11.9 ± 1.1	8.1 ± 1.2	0.007	10.8 ± 1.4	12.0 ± 2.4	0.413
20:0	33.9 ± 0.8	20.3 ± 2.3*	<0.001	27.3 ± 2.2	22.5 ± 2.5	0.193
22:0	54.6 ± 4.4	21.6 ± 4.1*	<0.001	29.6 ± 6.6	19.0 ± 3.6	0.276
22:1	27.5 ± 1.5	14.0 ± 2.3*	<0.001	18.0 ± 2.3	15.9 ± 2.1	0.593
23:0	70.1 ± 5.8	26.5 ± 5.7*	<0.001	32.0 ± 8.5	20.6 ± 5.2	0.395
23:1	50.0 ± 2.7	27.9 ± 4.1*	<0.001	30.1 ± 2.5	28.5 ± 3.5	0.765
24:0	67.2 ± 7.2	28.5 ± 5.4*	0.001	32.2 ± 8.3	17.8 ± 3.5	0.216
24:1	902.8 ± 61.8	356.3 ± 76.7*	<0.001	487.8 ± 108.1	307.5 ± 65.9	0.261
25:0	64.5 ± 3.0	35.0 ± 6.0*	<0.001	45.1 ± 4.8	37.5 ± 4.4	0.310
25:1	126.6 ± 9.0	58.2 ± 10.9*	<0.001	67.9 ± 11.2	51.5 ± 7.9	0.342
26:1	60.4 ± 4.9	26.1 ± 5.0*	<0.001	1.5 ± 5.3	21.8 ± 3.0	0.192
Total Ceramide	1927.9 ± 105.4	905.6 ± 162.0*	<0.001	1214.0 ± 192.2	894.8 ± 143.6	0.281

Values expressed as mean ± SE. P values represent the effect of group from multivariate analysis of covariance with region as the within subject factor and age and time since death as covariates. * indicates p value is still significant at the 0.05 level when further post hoc adjustment is done for the 26 individual comparisons using the Benjamini and Hochberg approach.

Supplementary Table 1. Grey matter sphingomyelin concentrations (nmol/g tissue wet weight) in anterior cingulate cortex (ACC) and occipital cortex (OCC) derived from control and Parkinson's disease (PD) cases.

SM(d18:1) acyl chain structure	ACC (Grey matter)					OCC (Grey matter)				
	Control		PD			Control		PD		
	Mean	SE	Mean	SE	p	Mean	SE	Mean	SE	p
14:0	18.2	1.2	8.5*	2.7	0.004	3.83	2.59	3.71	1.48	0.857
16:0	429.1	31.3	246.3*	22.0	<0.001	263.95	50.22	152.80	11.74	0.100
17:0	48.6	4.2	28.9*	3.4	0.002	33.39	5.46	22.25	1.95	0.111
18:0	3285.5	210.3	2007.2*	165.0	<0.001	1934.97	263.91	1445.91	110.56	0.140
18:1	293.6	19.4	249.9	16.2	0.060	181.33	23.12	168.75	25.45	0.889
20:0	337.6	24.1	386.4*	20.7	0.120	300.87	22.67	384.39	56.87	0.245
22:0	228.0	19.7	116.9*	13.4	<0.001	135.48	29.86	71.94	7.84	0.130
22:1	108.4	7.0	56.4*	7.4	<0.001	62.06	13.39	35.25	4.53	0.098
23:0	320.7	33.1	116.1*	19.7	<0.001	142.48	41.81	73.11	11.52	0.304
23:1	161.5	10.4	85.3*	13.8	0.001	91.76	20.88	56.80	8.95	0.191
24:0	450.6	67.7	186.8*	31.7	0.003	116.41	33.41	61.24	17.25	0.265
24:1	4021.5	358.7	1845.4*	348.7	0.001	2361.02	556.06	1191.14	193.84	0.107
25:0	129.3	25.1	65.0*	18.0	0.001	47.63	16.77	25.93	5.83	0.559
25:1	735.8	55.7	395.4*	70.7	<0.001	420.16	83.11	268.54	41.83	0.143
26:1	569.5	60.0	222.3*	40.7	0.001	307.32	64.12	178.25	21.94	0.140
Total SM	11628.2	877.2	6777.9*	1062.7	<0.001	6398.83	1165.82	4136.29	334.14	0.130

Values expressed as mean ± SE. P values represent the effect of group from multivariate analysis of covariance with region as the within subject factor and age and postmortem interval as covariates. * Indicates p value is still significant at the 0.05 level when further post hoc adjustment is done for the 26 individual comparisons using the Benjamini and Hochberg approach.

Supplementary Table 2. White matter ceramide concentrations (nmol/g tissue wet weight) in anterior cingulate cortex (ACC) and occipital cortex (OCC) derived from control and Parkinson's disease (PD) cases.

Cer(d18:1) acyl chain structure	ACC (White matter)					OCC (White matter)				
	Control		PD			Control		PD		
	Mean	SE	Mean	SE	p	Mean	SE	Mean	SE	p
16:0	14.8	3.4	20.4	2.1	0.425	29.9	5.7	56.8	16.5	0.207
18:0	46.9	4.3	42.4	4.1	0.804	58.2	8.3	140.1	40.0	0.028
18:1	615.7	73.6	736.5	108.9	0.312	886.3	76.6	626.3*	74.3	0.048
20:0	45.1	5.2	45.8	5.8	0.560	56.2	6.1	48.1	4.2	0.230
22:0	62.2	4.2	57.8	4.3	0.738	82.7	9.8	95.3	16.8	0.002
22:1	91.2	8.2	92.5	11.2	0.346	101.9	5.7	66.1*	7.5	0.978
23:0	113.9	9.6	106.4	7.9	0.824	143.5	19.4	110.9	16.5	0.031
23:1	114.7	11.4	120.6	17.8	0.366	116.1	6.4	81.9	12.2	0.141
24:0	1593.7	162.9	1548.1	168.4	0.409	1798.0	96.8	1228.7*	213.1	0.004
24:1	168.8	15.7	151.1	12.7	0.572	159.9	8.5	105.6	13.7	0.021
25:0	258.8	26.8	261.0	24.6	0.917	277.8	20.9	225.7	38.4	0.031
25:1	181.5	15.0	189.0	16.0	0.845	248.5	22.9	169.4	24.3	0.183
26:1	131.6	16.2	124.8	11.5	0.672	141.1	7.8	91.8*	11.8	0.003
Total Ceramide	3438.7	334.1	3496.4	375.6	0.730	4100.2	248.3	3046.7*	402.1	0.032

Values expressed as mean ± SE. P values represent the effect of group from multivariate analysis of covariance with region as the within subject factor and age and postmortem interval as covariates. * Indicates p value is still significant at the 0.05 level when further post hoc adjustment is done for the 26 individual comparisons using the Benjamini and Hochberg approach.

Supplementary Table 3. White matter sphingomyelin concentrations (nmol/g tissue wet weight) in anterior cingulate cortex (ACC) and occipital cortex (OCC) derived from control and Parkinson's disease (PD) cases.

SM(d18:1) acyl chain structure	ACC (White matter)					OCC (White matter)				
	Control		PD			Control		PD		
	Mean	SE	Mean	SE	p	Mean	SE	Mean	SE	p
14:0	12.3	3.2	18.7	2.7	0.554	24.0	4.5	6.6	3.4	0.015
16:0	543.3	17.3	553.6	26.2	0.968	791.2	55.4	505.7*	36.9	0.001
17:0	68.9	3.1	73.6	6.6	0.675	95.3	9.2	59.9	11.2	0.014
18:0	4090.4	170.4	4133.0	252.8	0.636	4939.7	237.8	3600.6*	209.0	0.001
18:1	315.3	13.2	339.5	23.0	0.642	342.7	22.4	305.5	14.6	0.139
20:0	350.5	20.2	321.5	14.0	0.308	283.7	19.2	376.6	26.1	0.017
22:0	348.8	26.5	327.4	20.7	0.445	333.6	25.4	251.5*	20.2	0.004
22:1	157.2	7.9	147.4	9.5	0.459	160.1	16.3	120.9	11.1	0.046
23:0	491.1	35.8	414.9	28.6	0.110	368.8	18.0	337.0	28.5	0.289
23:1	256.4	6.3	252.6	17.3	0.761	262.2	30.7	212.9	18.9	0.126
24:0	741.5	96.5	519.8	66.0	0.112	500.3	58.6	313.3	26.9	0.017
24:1	6356.5	277.6	5987.6	434.1	0.341	6398.8	546.1	4625.1	510.5	0.015
25:0	279.8	36.8	229.7	33.9	0.155	210.7	22.1	114.3	18.8	0.010
25:1	1168.6	53.4	1089.3	75.6	0.421	999.5	95.2	936.4	107.5	0.483
26:1	888.8	68.3	758.6	47.1	0.207	706.7	51.3	554.0	45.1	0.018
Total SM	16057.0	683.9	15123.1	760.6	0.249	16393.2	1009.5	12313.6*	949.4	0.005

Values expressed as mean ± SE. P values represent the effect of group from multivariate analysis of covariance with region as the within subject factor and age and postmortem interval as covariates. * Indicates p value is still significant at the 0.05 level when further post hoc adjustment is done for the 26 individual comparisons using the Benjamini and Hochberg approach.

Abbott et al. Figure 1

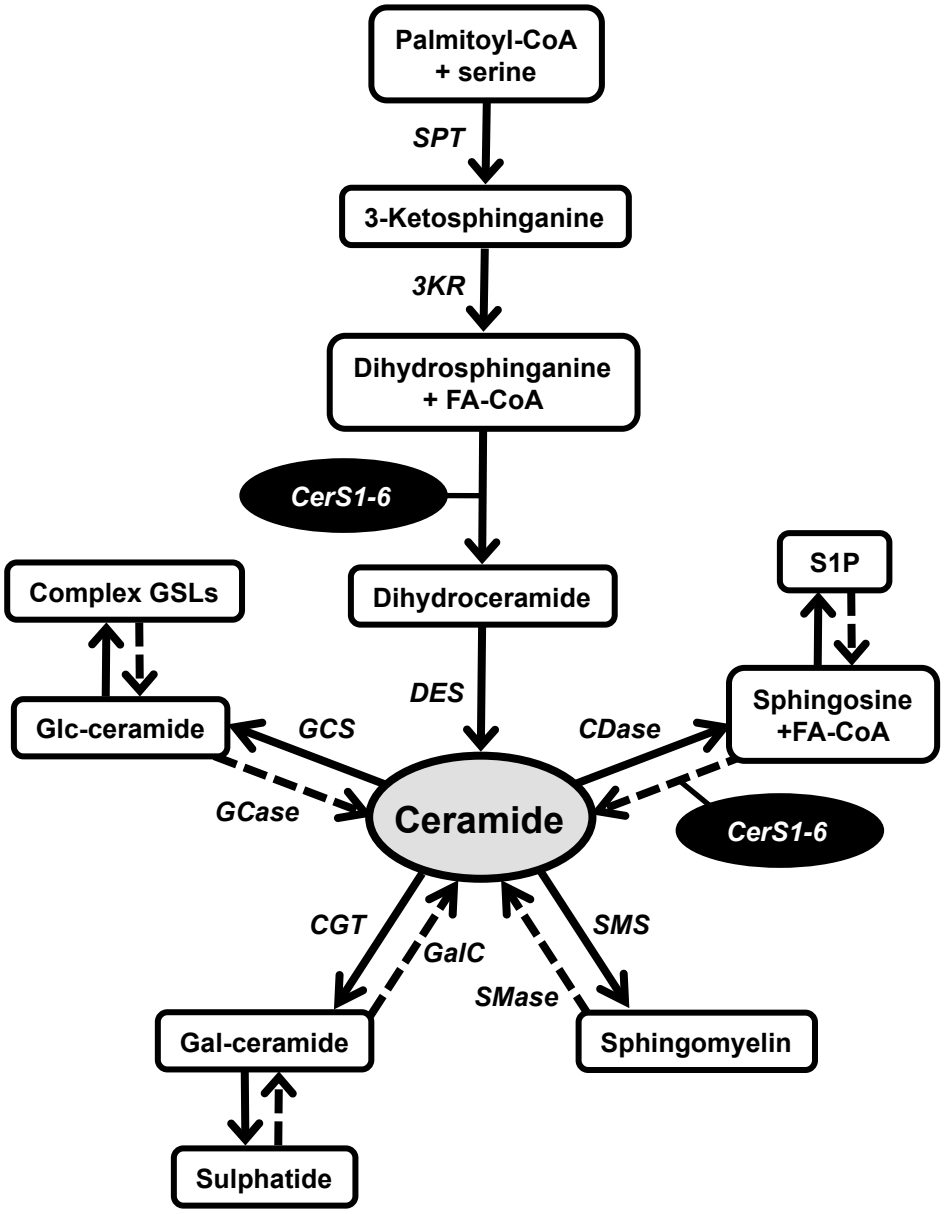

Abbott et al. Figure 2

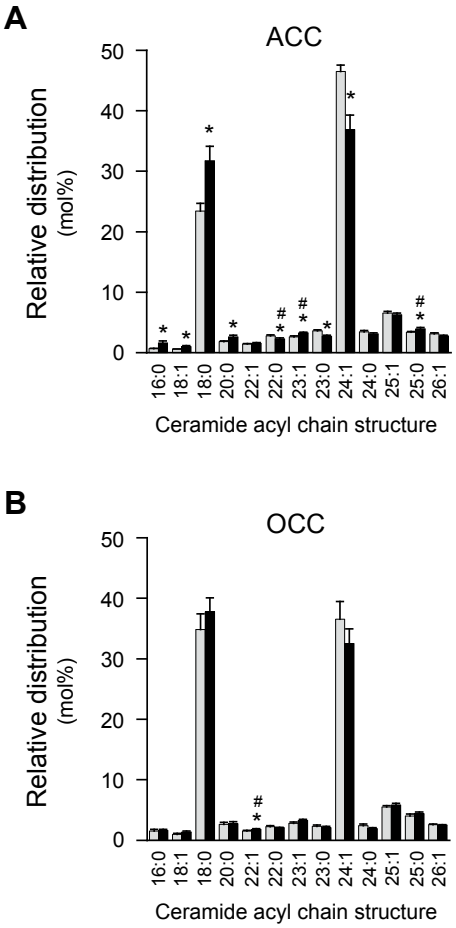

Abbott et al. Figure 3